

Sub-workspace design of binary manipulators using active and passive joints

Gang-Won Jang¹, Sang Jun Nam² and Yoon Young Kim^{2,*}

¹School of Mechanical Engineering, Kunsan National University, Kunsan, Chonbuk 573-701, Korea

²School of Mechanical and Aerospace Engineering and National Creative Research

Initiatives Center for Multiscale Design, Seoul National University
Shinlim-Dong, San 56-1, Kwanak-Gu, Seoul 151-742, Korea

(Manuscript Received April 24, 2007; Revised January 9, 2008; Accepted June 20, 2008)

Abstract

This paper is concerned with an efficient continuous variable optimization method for determining an optimal configuration of passive and active joints of a binary manipulator when it operates within a desired sub-workspace. When joints are passive, their states, either stretched or contracted, are also determined by the developed method. Manipulator operations in a sub-workspace can avoid unnecessary actuations, resulting in energy saving. A technique to increase the sub-workspace concentration degree for a given maximum number of allowable active joints is also suggested.

Keywords: Binary manipulator; Sub-workspace design; Active joint; Passive joint; Continuous-variable method

1. Introduction

A binary manipulator is a manipulator discretely actuated by a set of binary joints having two stable states. The workspace of a binary manipulator consists of a finite number of reachable points, which exponentially increases with the number of binary joints. Hyper-redundancy, high reliability and high task repeatability are the main advantages of binary manipulators over conventional manipulators having continuous joints, and these properties are favorable for manipulators operating in tough and complex work conditions. In addition, binary manipulators are cost-effective since two-state binary joints are generally inexpensive, and complex equipment for feedback control may be unnecessary.

The concept of manipulators consisting of discretely actuating joints and thus having discrete workspaces can be found in the early investigation of Pieper's planar serial digital manipulator [1]. With the

development of computers, the digital paradigm received attention [2, 3]. Chirikjian [4] introduced a hyper-redundant binary manipulator having large degrees of freedom and developed an optimal design method for simple pick-and-place tasks. They have also studied kinematic synthesis [4, 5], and inverse kinematics of binary manipulators [6]. In order to estimate the states of all binary joints for reaching a given target point, Ebert-Uphoff and Chirikjian [6] developed a method that can sequentially determine the configuration of a binary manipulator starting from a base module to maximize the discrete workspace density function [7]. Kim et al. have recently proposed the use of a continuous-variable-based optimization method for analysis of inverse kinematics [8]. Recent applications of binary manipulators can be found in space exploration robots [9-11].

In this paper, sub-workspace design problems for two-dimensional binary manipulators are considered. Because energy efficiency is an important issue especially for a battery-operated binary manipulator, its operation in a sub-workspace is preferred whenever possible. In this case, not all joints need to be actuated.

*Corresponding author. Tel.: +82 2 880 7154, Fax.: +82 2 872 5431
E-mail address: yykim@snu.ac.kr
© KSME & Springer 2008

Therefore, an efficient algorithm that can determine the states of all joints, passive or active, should be developed. For passive joints, the joint states, stretched or contracted, should be also determined. The algorithm must be fast enough to find the joint states in real time. Once a binary manipulator is designed, i.e., if the joint dimensions, the number of modules and their base lengths are determined, the workspace of a binary manipulator can be evaluated. A fast inverse kinematics algorithm [8] can be used to determine the states of joints (stretched or contracted) when a target location of an end-effector is given. However, if a binary manipulator needs to operate in a narrowed sub-workspace, not all joints need to be active. Thus the objective of this work is to find a method to identify active joint locations and determine states of remaining passive joints when the sub-workspace specified by the mean of a workspace density function and maximum number of active joints is given. To solve this problem, a technique to select a set of active joints yielding a desired workspace concentration degree also must be developed.

Two key ideas are proposed to develop a joint identification method. Firstly, an identification problem is set up as a “continuous-variable” based optimization problem. The use of continuous variables was proposed by Kim et al. for numerically efficient inverse kinematic analysis of binary manipulators [8]. By employing the same approach, the identification problem can be set up as an optimization problem of continuous variables, which can be applied with an efficient gradient-based optimizer. The second idea, which is a crucial idea, is to treat each joint length as a function of two variables. If the inverse kinematics were considered, only one variable for each joint length would be assigned. Two variables are introduced for every joint to distinguish whether each joint is an active or passive joint, and to identify either elongated or contracted states if the joint is passive. The detailed formulation will be given in section 3 and several sub-workspace design problems for two-dimensional binary manipulators are considered in section 4.

2. Workspace description

As a mean to describe the workspace of a binary manipulator, the workspace density function will be used [12]. Therefore, a brief introduction of the workspace density function will be presented here before the workspace design is considered.

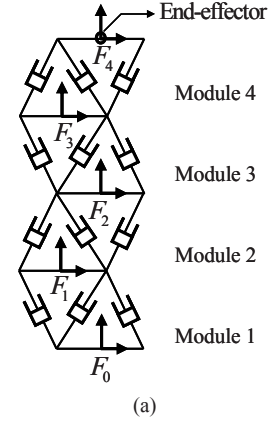
2.1 Workspace density function of a binary manipulator as a pdf

Fig. 1 shows a two-dimensional binary manipulator having four 3-bit prismatic joint modules. Because the joints of a manipulator have two binary states, the manipulator's workspace consists of a finite number of discrete points ($(2^3)^4 = 4,096$ points for the manipulator shown in Fig. 1). If K_i kinematic configurations are possible for the module i of a binary manipulator, the corresponding configuration set C_i can be written as

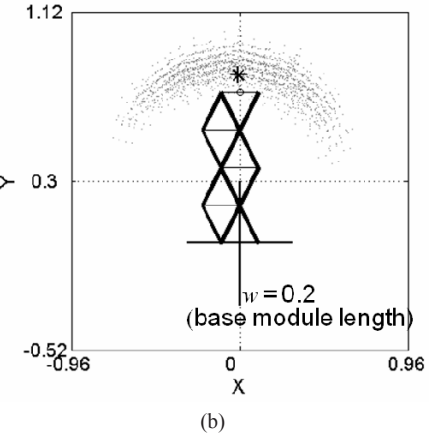
$$C_i = \{g_i^1, g_i^2, \dots, g_i^{K_i}\}, \quad (1a)$$

where

$$g_i^j = \begin{pmatrix} \mathbf{R}_i^j & \mathbf{b}_i^j \\ \mathbf{0} & 1 \end{pmatrix} \in SE(N). \quad (1b)$$



(a)



(b)

Fig. 1. (a) A binary manipulator with 4 3-bit modules, and (b) its workspace.

In Eq. (1b), \mathbf{R} is an N -dimensional rotation matrix (or an element of $SO(N)$), and \mathbf{b} is a position vector ($\mathbf{b} \in \mathbb{R}^N$). For convenience, g_i^j in Eq. (1b) may be written as $g_i^j = (\mathbf{b}_i^j, \mathbf{R}_i^j)$.

On the group of $SE(N)$, a normalized workspace density function ρ can be defined as a probabilistic density function (pdf) satisfying

$$\rho(g) \geq 0, \text{ and } \int_{SE(N)} \rho(g) dg = 1,$$

where g stands for a set of possible kinematic configurations. If a symbol $\rho_{i-1/i}$ is used to denote the pdf of the i -th module of a binary manipulator relative to the $(i-1)$ -th module, the pdf of the P -th module with respect to the base can be expressed as (see [13] for more details)

$$\rho_{0/P}(g) = (\rho_{0/1} * \rho_{1/2} * \dots * \rho_{P-1/P})(g), \quad (2)$$

where $*$ is a convolution operator defined as

$$(\rho_{i-1/i} * \rho_{i/i+1})(g) \triangleq \int_{SE(N)} \rho_{i-1/i}(h) \rho_{i/i+1}(h^{-1} \circ g) dh.$$

In Fig. 1(a), frames are attached on the bottom centers of the modules. If the transformation from the k -th frame of the manipulator to the i -th frame is denoted by $g_{i/k}$, the frame on the end-effector with respect to the base frame is written as

$$g_{0/P} = g_{0/1} \circ g_{1/2} \circ \dots \circ g_{P-1/P}. \quad (3)$$

The inverse kinematics of a binary manipulator is a problem for finding the states of all binary joints which match the end-effector to a specific target frame as close as possible. The configuration of the i -th module is determined by maximizing $\rho_{i/P}$ of the target. Thus, using Eq. (3) and pdf's obtained from Eq. (2) and first determining $g_{0/1}$ by maximizing $\rho_{1/P}$ of the target, the configuration of the next higher modules can be found consecutively [6].

2.2 Mean of the workspace density function

In order to design the workspace of a binary manipulator, a mean value of $\rho(g)$, a statistical property, may be used instead of using $\rho(g)$ directly. The mean value of $\rho(g)$ (denoted by g^m) can be found as the solution that minimizes the function

$F(g_1)$ such that

$$F(g_1) = \int_{SE(N)} (D(g_1, g_2))^2 \rho(g_2) dg_2 \quad (4)$$

$$= \int_{\mathbb{R}^N} \int_{SO(N)} \left(\|\mathbf{b}_1 - \mathbf{b}_2\|_2^2 + L^2 \|\mathbf{R}_1 - \mathbf{R}_2\|_2^2 \right) \rho(\mathbf{b}_2, \mathbf{R}_2) d\mathbf{b}_2 d\mathbf{R}_2$$

subject to $\mathbf{b}_1 \in \mathbb{R}^N$ and $\mathbf{R}_1 \in SO(N)$.

For later use, we explicitly define the metric D in Eq. (4) (see [12, 14])

$$D(g_1, g_2) = \sqrt{\|\mathbf{b}_1 - \mathbf{b}_2\|_2^2 + L^2 \|\mathbf{R}_1 - \mathbf{R}_2\|_2^2}, \quad (5)$$

where $L \in \mathbb{R}^+$ is a unit-matching parameter.

Suthakorn and Chirikjian [12] showed that \mathbf{b}^m and \mathbf{R}^m can be obtained simply by calculating the averages of the translational part and rotational part of all kinematic configurations, respectively:

$$\mathbf{b}^m = \int_{\mathbb{R}^N} \mathbf{b} \left(\int_{SO(N)} \rho(\mathbf{b}, \mathbf{R}) d\mathbf{R} \right) d\mathbf{b}, \quad (6a)$$

$$\mathbf{R}^m = \mathbf{M} (\mathbf{M}^T \mathbf{M})^{-1/2}, \quad (6b)$$

where

$$\mathbf{M} = \int_{SO(N)} \mathbf{R} \left(\int_{\mathbb{R}^N} \rho(\mathbf{b}, \mathbf{R}) d\mathbf{b} \right) d\mathbf{R}. \quad (6c)$$

Because \mathbf{M} in Eq. (6c) is not included in $SO(N)$, \mathbf{R}^m is taken to be the closest rotation matrix to \mathbf{M} in Eq. (6b). The mean of the i -th module in Fig. 1(a), for example, can be found by considering eight configurations of the three binary joints $\{g_i^1, g_i^2, \dots, g_i^8\}$. Using Eq. (6), the mean position and the mean rotation of the module are

$$\mathbf{b}_i^m = \sum_{k=1}^8 \mathbf{b}_i^k \rho^k \quad \text{and} \quad \mathbf{R}_i^m = \mathbf{M}_i (\mathbf{M}_i^T \mathbf{M}_i)^{-1/2}, \quad (7a)$$

where

$$\mathbf{M}_i = \sum_{k=1}^8 \mathbf{R}_i^k \rho^k. \quad (7b)$$

In Eq. (7), ρ^k for all k 's is taken to be $1/8$.

The pdf of two concatenated modules having $\rho_i(g)$ and $\rho_{i+1}(g)$ has the following mean position $\mathbf{b}_{i*(i+1)}^m$ and the mean rotation $\mathbf{R}_{i*(i+1)}^m$: (see [12] for

the derivation)

$$\mathbf{b}_{i*(i+1)}^m \triangleq \mathbf{b}_i^m + \mathbf{M}_i \mathbf{b}_{i+1}^m, \quad (8a)$$

$$\mathbf{R}_{i*(i+1)}^m \triangleq \mathbf{M}_{i*(i+1)} \left(\mathbf{M}_{i*(i+1)}^T \mathbf{M}_{i*(i+1)} \right)^{-1/2}, \quad (8b)$$

where

$$\mathbf{M}_{i*(i+1)} \triangleq \mathbf{M}_i \mathbf{M}_{i+1}. \quad (8c)$$

Thus the mean position of the workspace of the manipulator having P modules is given as

$$\mathbf{b}_{1*2*...*P}^m = \mathbf{b}_1^m + \sum_{i=1}^{P-1} \left(\prod_{j=1}^i \mathbf{M}_j \right) \mathbf{b}_{i+1}^m, \quad P \geq 2. \quad (9)$$

Because the mean of rotation $\mathbf{R}_{1*2*...*P}^m$ lacks practical meaning, it will not be considered in workspace design.

3. Sub-workspace design of binary manipulator

3.1 Formulation

A sub-workspace is a subset of the workspace of a given binary manipulator (which will be referred to as a design-domain manipulator). By constraining the number of active joints of the manipulator, various sub-workspaces can be obtained. The design target is to obtain the sub-workspace whose mean position lies at the specified location for a given number of active joints. In the design process, a technique to control the degree of workspace concentration will be also developed. In this paper, the workspace design problem to determine the active and passive joint sets is formulated as

$$\text{Find } \mathbf{r} = \{r_{1,1}, r_{1,2}, r_{1,3}, \dots, r_{i,j}, \dots, r_{P,1}, r_{P,2}, r_{P,3}\} \quad (10a)$$

$$\text{minimizing } D(\mathbf{b}^m, \bar{\mathbf{b}}), \quad (10b)$$

$$\text{subject to } N_A \leq \bar{N}_A \leq 3P \quad (10c)$$

where $r_{i,j}$ in Eq. (10a) denotes the states of the j -th joint of the i -th module of a given binary manipulator. The states variable $r_{i,j}$ is the design variable of the above minimization problem and can have one of the three states:

- $r_{i,j} = r_A$: the joint is active, i.e., an actuator.
- $r_{i,j} = r_{p-\min}$: the joint is passive at a contracted states.

- $r_{i,j} = r_{p-\max}$: the joint is passive at a stretched states.

In Eq. (10b), \mathbf{b}^m is the mean position of the subspace under design and $\bar{\mathbf{b}}$ is the desired mean position. The total number of allowable joints is limited by Eq. (10c).

3.2 Optimization in a continuous variable space

In the optimization problem formulated by Eq. (10), the design variables are discrete, i.e., $r_{i,j} = r_A$, r_{p-L} or r_{p-H} . The optimization involving discrete design variables may be directly solved by employing non-gradient-based optimizers such as a genetic algorithm. However, a recent investigation has shown that inverse kinematics of binary manipulators can be solved efficiently in a continuous variable design space even for a large number of modules [8]. The method to convert a discrete-variable inverse kinematics problem into a continuous variable optimization problem is given in [8]. Specifically, the variable $q_{i,j}$ (the length of the i -th joint of the j -th module) converging to either q^{\min} (contracted length) or q^{\max} (stretched length) at the end of optimization was introduced. Motivated by the success in the inverse kinematics, we considered solving the optimization in Eq. (10) in a continuous variable space by using a fast gradient-based optimizer. The fast computation is important for real time operation of a binary manipulator. The main issue is the expression method of discrete joint states by using continuous design variables. To this end, we propose to control the upper and lower bounds of the joint length $q_{i,j}$ by introducing two continuous variables $c_{i,j}$ and $d_{i,j}$ such that

$$\min(c_{i,j}, d_{i,j}) \leq q_{i,j} \leq \max(c_{i,j}, d_{i,j}),$$

$$q^{\min} \leq c_{i,j}, d_{i,j} \leq q^{\max} \quad (i=1, \dots, P \text{ and } j=1, 2, 3).$$

Assuming that continuous variables $c_{i,j}$ and $d_{i,j}$ converge to either q^{\min} or q^{\max} at the end of the workspace design, four combinations of $c_{i,j}$ and $d_{i,j}$ in Table 1 are possible. If $c_{i,j} = d_{i,j}$, $q_{i,j}$ becomes a constant and the corresponding joint becomes a passive joint. If $c_{i,j} \neq d_{i,j}$, $q_{i,j}$ can vary between q^{\min} and q^{\max} , so the corresponding joint becomes an active joint.

Table 1. Joint states depending on the values of c_{ij} and d_{ij}

$c_{i,j}$	$d_{i,j}$	$q_{i,j}$	Joint states
q^{\max}	q^{\max}	$q^{\max} \leq q_{i,j} \leq q^{\max}$	$r_{p,\max}$ (passive, stretched)
q^{\max}	q^{\min}	$q^{\min} \leq q_{i,j} \leq q^{\max}$	r_A (active)
q^{\min}	q^{\max}	$q^{\min} \leq q_{i,j} \leq q^{\max}$	r_A (active)
q^{\min}	q^{\min}	$q^{\min} \leq q_{i,j} \leq q^{\min}$	$r_{p,\min}$ (passive, contracted)

The next step is to find the values of $c_{i,j}$ and $d_{i,j}$ yielding the specified sub-workspace and to make $c_{i,j}$ and $d_{i,j}$ approach q^{\min} or q^{\max} . The following is the proposed optimization formulation :

$$\text{Find } \mathbf{c} = \{c_{1,1}, c_{1,2}, c_{1,3}, \dots, c_{P,1}, c_{P,2}, c_{P,3}\}, \quad (11a)$$

$$\mathbf{d} = \{d_{1,1}, d_{1,2}, d_{1,3}, \dots, d_{P,1}, d_{P,2}, d_{P,3}\},$$

minimizing

$$f = \sum_{i=1}^P \sum_{j=1}^3 \beta_i \{ (q^{\max} - c_{i,j})(c_{i,j} - q^{\min}) + (q^{\max} - d_{i,j})(d_{i,j} - q^{\min}) \}, \quad (11b)$$

$$\text{subject to } g_1 = D(\mathbf{b}^m, \bar{\mathbf{b}}) - \varepsilon \leq 0, \quad (11c)$$

$$g_2 = \sum_{i=1}^P \sum_{j=1}^3 \left(\frac{c_{i,j} - d_{i,j}}{q^{\max} - q^{\min}} \right)^2 - \bar{N}_A = 0, \quad (11d)$$

$$q^{\min} \leq c_{i,j}, d_{i,j} \leq q^{\max} \quad (i=1,2,\dots,P \text{ and } j=1,2,3). \quad (11e)$$

The role of the objective function f in Eq. (11b) is to force $c_{i,j}$ and $d_{i,j}$ to converge to either q^{\min} or q^{\max} . If $c_{i,j}$ and $d_{i,j}$ take some intermediate values between q^{\min} and q^{\max} , it is not possible to determine the joint states. The position of a sub-workspace's mean is controlled through the constraint in Eq. (11c), where ε is a user-defined small parameter. One may use g_1 as the objective function and replace the minimization condition in Eq. (11b) as a design constraint. In this case, however, the obtained solutions were often local optimal solutions that did not take \mathbf{b}^m sufficiently close to $\bar{\mathbf{b}}$. The symbol β_i in Eq. 11 (b) is the weighting parameter introduced to control the locations of active joints and thus the concentration degree of the designed workspace. Two typical forms of β_i are

$$\beta_i = i^n, \quad (12a)$$

$$\beta_i = (P - i + 1)^n, \quad (12b)$$

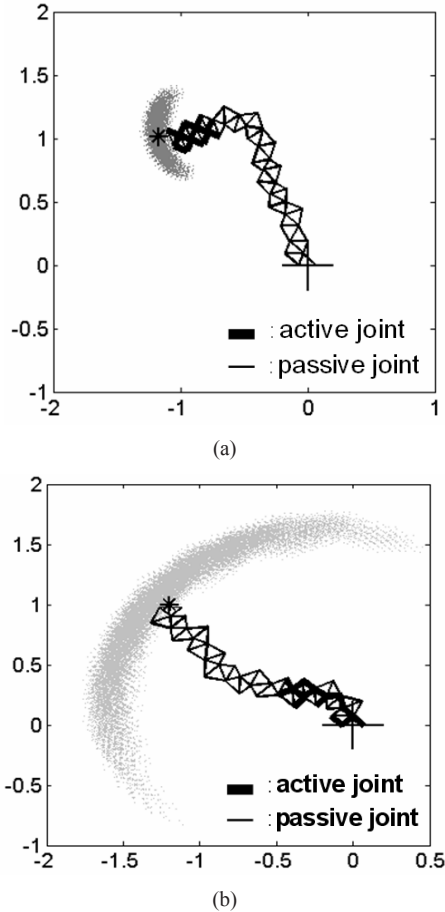


Fig. 2. Comparison of the degree of concentration of the sub-workspaces designed by using (a) $\beta_i = i^n$ (Eq. (12a)) and (b) $\beta_i = (P - i + 1)^n$ (Eq. (12b)). (Assumption: the same manipulator, the same number of active joint ($N_A = 14$), and the same workspace center).

where n is usually taken as a value between 0 and 5.

Assume that two manipulators have the same number of modules, the same number of active joints, and the same mean of the workspaces. The degree of workspace concentration, however, can be considerably different depending on the locations of the active actuators. If larger weighting factors are used on the upper modules, i.e., if Eq. (12a) is used, the proposed workspace design formulation given in Eq. (11) tends to distribute active joints in the upper modules. The sub-workspace designed by using Eq. (12a) is shown in Fig. 2(a), which is compared with the sub-workspace in Fig. 2(b) designed by using (12b). On the other hand, the use of larger weighing factors in lower modules resulted in the appearance of active joints in lower modules. Because the variables $c_{i,j}$

and $d_{i,j}$ of lower modules contribute greatly to the magnitude of the objective function, these variables tend to reach q^{\min} and q^{\max} faster than those of higher modules during the optimization process. Furthermore, to satisfy the constraint on the number of active joints in (11d), $c_{i,j}$ and $d_{i,j}$ of the lower modules tend to approach the states of active joints. Thus, the parameter β_i can be used to control the concentration degree of the designed workspace.

Although Eq. (11b) certainly pushes $c_{i,j}$ and $d_{i,j}$ towards q^{\min} and q^{\max} , $c_{i,j}$ and $d_{i,j}$ are not discrete values. Therefore, a post-processing to replace the values of $c_{i,j}$ and $d_{i,j}$ by their closest lower and upper bounds is needed. If intermediate values of $c_{i,j}$ and $d_{i,j}$ are obtained in lower modules, in particular, the post-processing may move the mean of the designed sub-workspace to a point quite off from the given mean. The same problem was observed in solving the inverse kinematics of a binary manipulator [8]. To avoid intermediate values of $c_{i,j}$ and $d_{i,j}$, the following nonlinear S-shape mapping functions pushing $c_{i,j}$ and $d_{i,j}$ closer to q^{\min} or q^{\max} is introduced.

$$c_{i,j} = \frac{q^{\max} - q^{\min}}{1 + \exp(-t \cdot p_{i,j}^c)} + q^{\min}, \quad (13a)$$

$$d_{i,j} = \frac{q^{\max} - q^{\min}}{1 + \exp(-t \cdot p_{i,j}^d)} + q^{\min}, \quad (13b)$$

$$t \in \mathbb{R}^+ \text{ and } p^{\min} \leq p_{i,j}^c, p_{i,j}^d \leq p^{\max} \quad (13c)$$

In Eq. (13), $p_{i,j}^c$ and $p_{i,j}^d$ are new design variables, and the optimization problem set up by Eq. (11) is then solved for $p_{i,j}^c$ and $p_{i,j}^d$. For all problems solved in this work, we used $p^{\min} = -100$, $p^{\max} = 100$ and $t = 0.25$. Since the S-shaped mapping functions in Eq. (13a, b) have higher sensitivities for the intermediate values of $c_{i,j}$ and $d_{i,j}$ (i.e., values near $(q^{\min} + q^{\max})/2$), the intermediate values can be pushed more efficiently towards either q^{\min} or q^{\max} . Some numerical tests on the effect of the S-shape nonlinear function can be found in [8, 15, 16].

Fig. 3 illustrates the overall process of the proposed optimization-based method for designing the sub-workspace of a binary manipulator. For the optimization, an efficient gradient-based method, MMA (method of moving asymptotes) [17], was used. The optimizer requires information of the sensitivities of f , g_1 and g_2 . The following is the required sensi-

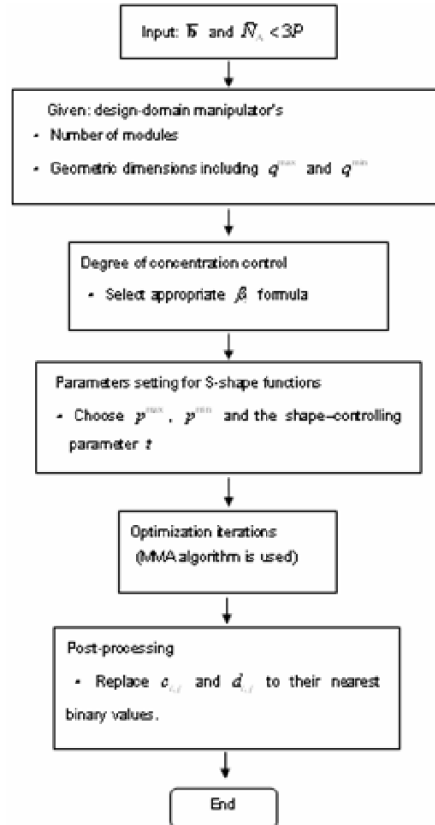


Fig. 3. A schematic description of the proposed optimization-based method for the sub-workspace design of a binary manipulator.

tivity analysis. The sensitivity of g_1 with respect to the auxiliary design variables $p_{i,j}^\alpha$ ($\alpha = c$ or d) is

$$\begin{aligned} \frac{dg_1}{dp_{i,j}^\alpha} = & \frac{\partial}{\partial \alpha_{i,j}} D(\mathbf{b}^m, \bar{\mathbf{b}}) \frac{\partial \alpha_{i,j}}{\partial p_{i,j}^\alpha} = \frac{\partial}{\partial \alpha_{i,j}} D(\mathbf{b}^m, \bar{\mathbf{b}}) \\ & \times \frac{t(q^{\max} - q^{\min}) \exp(-t \cdot p_{i,j}^\alpha)}{\{1 + \exp(-t \cdot p_{i,j}^\alpha)\}^2} \end{aligned} \quad (\alpha = c \text{ or } d) \quad (14)$$

The partial derivative, $dD/d\alpha_{i,j}$, can be easily found if $d\mathbf{b}^m/dq_{i,j}^\alpha$ is known. Differentiating Eq. (9) yields

$$\begin{aligned} \frac{\partial \mathbf{b}^m}{\partial q_{i,j}^\alpha} = & \left(\prod_{m=1}^{i-1} \mathbf{M}_m \right) \frac{\partial \mathbf{b}^i}{\partial q_{i,j}^\alpha} \\ & + \sum_{m=i+1}^P \left(\prod_{n=1}^{i-1} \mathbf{M}_n \right) \frac{\partial \mathbf{M}_i}{\partial q_{i,j}^\alpha} \left(\prod_{n=i+1}^{m-1} \mathbf{M}_n \right) \mathbf{b}^m, \end{aligned} \quad (15)$$

where $\partial \mathbf{b}^i / \partial q_{i,j}^\alpha$ and $\partial \mathbf{M}_i / \partial q_{i,j}^\alpha$ can be explicitly calculated by using Eq. (7).

The sensitivities of f and g_2 with respect to $p_{i,j}^\alpha$ are obtained as

$$\begin{aligned} \frac{df}{dp_{i,j}^\alpha} &= \beta_i(q^{\max} + q^{\min} - 2q_{i,j}^\alpha) \\ &\times \frac{t(q^{\max} - q^{\min})\exp(-t \cdot p_{i,j}^\alpha)}{\{1 + \exp(-t \cdot p_{i,j}^\alpha)\}^2}, \end{aligned} \quad (16)$$

$$\begin{aligned} \frac{dg_2}{dp_{i,j}^\alpha} &= 2 \frac{q_{i,j}^m - q_{i,j}^n}{(q^{\max} - q^{\min})^2} \\ &\times \frac{t(q^{\max} - q^{\min})\exp(-t \cdot p_{i,j}^\alpha)}{\{1 + \exp(-t \cdot p_{i,j}^\alpha)\}^2}. \end{aligned} \quad (17)$$

If one does not use the sensitivity analysis given in Eqs. (15-17), the sensitivities should be calculated by the finite difference method, which is very time-consuming.

Because of hyper redundancy of a binary manipulator and the local minima property of the gradient-based optimizer, the obtained configuration of a binary manipulator having a specific sub-workspace may not be the global minimum. Strict constraint on the closeness parameter in (11c) reduces the redundancy, but a too small value of the parameter can introduce the ill-posedness of the optimization problem.

Table 2. The states of binary joints for each work area (The symbols \mathbf{A} , P_{\max} and P_{\min} refer to r_A , $r_{P_{\max}}$ and $r_{P_{\min}}$, respectively.).

Work point	Module index																			
	1	2	3	4	5	6	7	8	9	10	11	12	13	14	15	16	17	18	19	20
(0.8, 0.2)	P_{\max}	P_{\max}	P_{\min}	P_{\min}	P_{\max}	P_{\max}	P_{\min}	P_{\min}	P_{\max}	P_{\min}	P_{\max}	P_{\min}	P_{\max}	P_{\max}	A	A	A	A	A	
	P_{\min}	P_{\min}	P_{\max}	P_{\min}	P_{\max}	P_{\min}	P_{\min}	P_{\max}	P_{\min}	P_{\min}	P_{\min}	P_{\max}	P_{\min}	P_{\min}	A	A	A	A	A	
	P_{\min}	P_{\min}	P_{\min}	P_{\max}	P_{\max}	P_{\min}	P_{\min}	P_{\min}	P_{\max}	P_{\min}	P_{\min}	P_{\min}	P_{\min}	P_{\min}	A	A	A	A	A	
(0.5, 0.9)	P_{\max}	P_{\max}	P_{\max}	P_{\max}	P_{\min}	P_{\min}	P_{\min}	P_{\min}	P_{\max}	P_{\min}	P_{\max}	P_{\min}	P_{\max}	P_{\max}	A	A	A	A	A	
	P_{\max}	P_{\max}	P_{\min}	P_{\min}	P_{\min}	P_{\max}	P_{\max}	P_{\max}	P_{\min}	P_{\min}	P_{\max}	P_{\min}	P_{\min}	P_{\min}	A	A	A	A	A	
	P_{\min}	P_{\min}	P_{\max}	P_{\min}	P_{\max}	P_{\min}	P_{\max}	P_{\min}	A	A	A	A	A							
(-0.1, 1.1)	P_{\max}	P_{\min}	P_{\min}	P_{\min}	P_{\min}	P_{\max}	P_{\max}	P_{\max}	P_{\min}	P_{\min}	P_{\min}	P_{\max}	P_{\min}	P_{\max}	A	A	A	A	A	
	P_{\max}	P_{\max}	P_{\max}	P_{\max}	P_{\max}	P_{\min}	P_{\min}	P_{\min}	P_{\max}	P_{\min}	P_{\min}	P_{\min}	P_{\min}	P_{\min}	A	A	A	A	A	
	P_{\min}	P_{\max}	P_{\min}	P_{\max}	P_{\max}	P_{\min}	P_{\min}	P_{\min}	P_{\max}	P_{\min}	P_{\min}	P_{\min}	P_{\min}	P_{\min}	A	A	A	A	A	
(-0.8, 0.5)	P_{\max}	P_{\min}	P_{\max}	P_{\min}	P_{\min}	P_{\min}	P_{\max}	P_{\max}	P_{\min}	P_{\min}	P_{\max}	P_{\min}	P_{\max}	P_{\max}	A	A	A	A	A	
	P_{\min}	P_{\max}	P_{\min}	P_{\max}	P_{\max}	P_{\min}	P_{\min}	P_{\min}	P_{\max}	P_{\min}	P_{\min}	P_{\min}	P_{\min}	P_{\min}	A	A	A	A	A	
	P_{\max}	P_{\max}	P_{\max}	P_{\max}	P_{\max}	P_{\min}	P_{\min}	P_{\min}	P_{\max}	P_{\min}	P_{\min}	P_{\min}	P_{\min}	P_{\min}	A	A	A	A	A	
(-0.7, -0.4)	P_{\max}	P_{\min}	P_{\min}	P_{\min}	P_{\max}	P_{\min}	P_{\max}	P_{\min}	P_{\min}	P_{\min}	P_{\max}	P_{\max}	P_{\max}	P_{\max}	A	A	A	A	A	
	P_{\min}	P_{\min}	P_{\max}	P_{\max}	P_{\max}	P_{\min}	P_{\max}	P_{\max}	P_{\min}	P_{\max}	P_{\min}	P_{\max}	P_{\max}	P_{\max}	A	A	A	A	A	
	P_{\max}	P_{\max}	P_{\max}	P_{\max}	P_{\max}	P_{\min}	P_{\min}	P_{\min}	P_{\max}	P_{\min}	P_{\max}	P_{\max}	P_{\max}	P_{\max}	A	A	A	A	A	

4. Numerical examples

A two-dimensional binary manipulator having 20 3-bit modules is considered as a given manipulator, whose workspace is illustrated in Fig. 4. Five subworkspace mean positions, $\bar{\mathbf{b}}_k$ ($k = 1, 2, \dots, 5$), marked in Fig. 4, will be considered. For the subworkspace design, only 15 joints will be used as active joints among 60 joints of the given manipulator. The dimensions of the modules are $q^{\min} = 0.06$, $q^{\max} = 0.08$, and the base length $w = 0.06$ (see Fig. 1). The closeness controlling parameter ε in Eq.

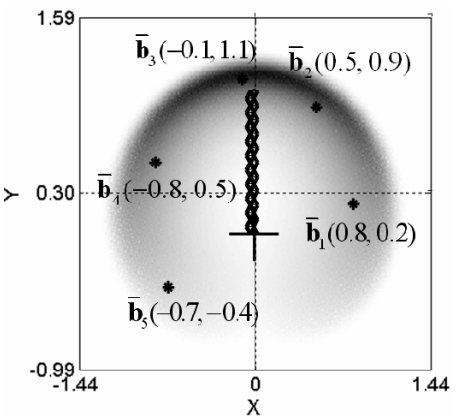


Fig. 4. The full workspace of a binary manipulator having 20 modules (The symbols * indicate the desired centers of sub-workspaces.)

Table 3. DOC's around the desired mean position \bar{b}_k and around the actual mean position \bar{b}_k^* of the designed sub-workspace (DOC = Degree of Concentration).

	\bar{b}_1	\bar{b}_2	\bar{b}_3	\bar{b}_4	\bar{b}_5
Given \bar{b}_k	(0.8,0.2)	(0.5,0.9)	(-0.1,1.1)	(-0.8,0.5)	(-0.7,-0.4)
DOC around \bar{b}_k	19974	19702	19232	20282	19892
Calculated \bar{b}_k^*	(0.79,0.22)	(0.47,0.91)	(-0.06,1.09)	(-0.80,0.51)	(-0.70,-0.37)
DOC around \bar{b}_k^*	20460	20460	20460	20460	20460

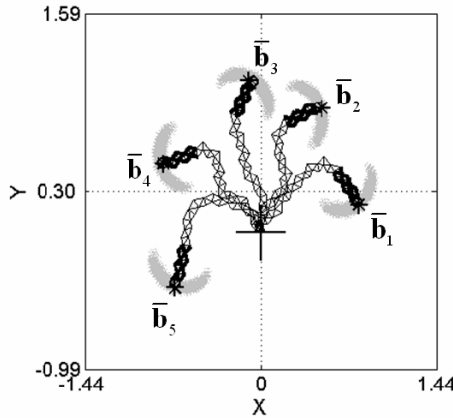


Fig. 5. Sub-workspaces by using $\beta_i = i^4$ (thick lines: active joints, thin lines: passive joints).

(11c) is set to 0.01. To maximize the degree of concentration of the sub-workspace around \bar{b}_k , $\beta_i = i^4$ in Eq. (12a) is selected.

Table 2 lists the joint states for each designed sub-workspace. Because $\beta_i = i^4$ were used, as shown in the table, the active joints were placed in upper modules. Table 3 lists the degrees of concentration of the sub-workspaces on point \bar{b}_k , which is defined as

$$\text{DOC} = \text{number of reachable points on } \Omega_{\bar{b}_k},$$

where $\Omega_{\bar{b}_k}$ is a circle centered at \bar{b}_k . The radius of $\Omega_{\bar{b}_k}$ is set to 0.1 in this example. In Table 3, \bar{b}_k^* is the actual mean position of the optimized sub-workspace. Table 3 shows that the passive joint states are so selected to make \bar{b}_k^* as close as possible to the desired \bar{b}_k . Fig. 5 shows the designed sub-workspaces, where the joints drawn in thick lines denote active joints and those in thin lines, passive joints. If the mean positions of sub-workspaces move sequentially, from \bar{b}_1 to \bar{b}_2 for instance, only the states of passive joints located in the lower modules

Table 4. The effects of the weight β_i on the sub-workspace characteristics.

	Given $\bar{b}_1 = (0.8, 0.2)$	Given $\bar{b}_4 = (-0.8, 0.5)$
$\beta_i = i^4$	DOC=20460	DOC=20460
$\beta_i = (P-i+1)^n$	DOC=4442	DOC=2051

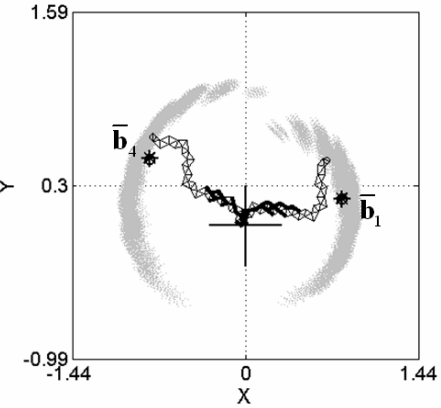


Fig. 6. The sub-workspaces by using $\beta_i = (P-i+1)^4$. (thick lines: active joints, thin lines: passive joints).

need to be changed. In this case, the proposed optimization-based sub-workspace design algorithm can be also implemented efficiently by minimizing the movements of the passive joints.

The effect of β_i on the configuration of the sub-workspace is investigated by examining DOC. Even if the same \bar{b} is given, considerably different DOC's can be obtained if different β_i 's are used. For the same target points \bar{b}_1 and \bar{b}_4 shown in Fig. 4, the sub-workspace design problem is solved by using $\beta_i = (P+1-i)^4|_{P=20} = (21-i)^4$. Because more weights are given on the joints of lower modules, the active joints appear in the lower modules. Consequently, the sub-workspaces in Fig. 6 are wider and less dense, resulting in less precision around the desired positions than those in Fig. 5. The degrees of concentration for the results obtained by using $\beta_i = i^4$ and $\beta_i = (21-i)^4$ are compared in Table 4. The use of β_i in Eq. (12b) seems to be adequate for designing manipulators required to have a wide work area where rough precision is acceptable. Thus, depending on the desired precision within the workspace area, one may choose an appropriate weighting parameter β_i . The exponent n in Eq. (12) also affects the location of active joints, but $n=4$ seems to yield satisfactory results.

5. Conclusions

A systematic configuration method to determine the joint states of a binary manipulator with only a small number of active joints is developed for operation of the manipulator within a sub-workspace. The proposed method is formulated as an optimization problem in a continuous variable design space where the objective is to minimize the distance between the mean of the designed sub-workspace and the prescribed sub-workspace center. Using two design variables to control the length of each joint was effective in determining the locations of active and passive joints. If a joint became a passive joint, the joint state, either contracted or stretched, is also determined during the optimization iteration. A weighting parameter method efficiently controlled the location of active joints and thus the degree of the workspace concentration.

Acknowledgments

The first author was supported by the Kunsan National University's Academic Support Program in the year 2005. The second and third authors were supported by the National Creative Research Initiatives Program (the Korea Science and Technology Foundation grant No. 2007-019) contracted the institute of Advanced Machinery and Design at Seoul National University.

References

- [1] D. L. Pieper, The kinematics of manipulators under computer control, PhD Dissertation, Stanford University, (1968).
- [2] V. C. Anderson and R. C. Horn, Tensor arm manipulator design, *ASME Transactions*, 67-DE-57 (1967) 1-12.
- [3] B. Roth, J. Rastegar and V. Scheinman, On the design of computer controlled manipulators, in Proc. 1st CISM-IFTMM Symp. Theory and Practice Robots and Manipulators, (1973).
- [4] G. S. Chirikjian, Kinematic synthesis of mechanisms and robotic manipulators with binary actuators, *ASME J. Mech. Design*, vol. 117 (1995) 573-580.
- [5] A. B. Kyatkin and G. S. Chirikjian, Synthesis of binary manipulators using the Fourier transform on the Euclidean group, *ASME J. Mech. Design*, vol. 121 (1999) 9-14.
- [6] I. Ebert-Uphoff and G. S. Chirikjian, Inverse kinematics of discretely actuated hyperredundant manipulators using workspace densities, in Proc. IEEE Int. Conf. on Robotics and Automation (1996) 139-145.
- [7] I. Ebert-Uphoff and G. S. Chirikjian, Efficient workspace generation for binary manipulators with many actuators, *J. Robotic Syst.*, 12 (6) (1995) 383-400.
- [8] Y. Y. Kim, G. W. Jang and S. J. Nam, Inverse kinematics of binary manipulators by using the continuous-variable-based optimization method, *IEEE Transactions on Robotics*, 22 (1) (2006) 33-42.
- [9] E. Paljug, T. Ohm and S. Hayati, The JPL serpentine robot: a 12 dof system for inspection, in Proc. IEEE Int. Conf. on Robotics and Automation (1995) 3143-3248.
- [10] M. D. Lichter, V. A. Sujan and S. Dubowsky, Computational issues in the planning and kinematics of binary robots, in Proc. Int. Conf. Robotics and Automation, Washington DC, (2002).
- [11] V. A. Sujan, M. D. Lichter and S. Dubowsky, Lightweight hyper-redundant binary elements for planetary exploration robots, in Proc. IEEE/ASME Int. Conf. Advanced Intelligent Mechatronics (2001) 1273-1278.
- [12] J. Suthakorn and G. S. Chirikjian, A new inverse kinematics algorithm for binary manipulators with many actuators, *Advanced Robotics*, 15 (2) (2001) 225-244.
- [13] G. S. Chirikjian and I. Ebert-Uphoff, Numerical convolution on the Euclidean group with applications to workspace generation, *IEEE Trans. Robotics Automat.*, 14 (1) (1998) 123-136.
- [14] G. S. Chirikjian and A. B. Kyatkin, Engineering applications of noncommutative harmonic analysis, CRC Press, Ann Arbor, MI, (2000).
- [15] Y. Y. Kim and G. H. Yoon, Multi-resolution multi-scale topology optimization – a new paradigm, *International Journal of Solids and Structures*, 37 (2000) 5529-5559.
- [16] G. H. Yoon and Y. Y. Kim, The role of S-shaped mapping functions in the SIMP approach for topology optimization, *KSME Int. J.*, 15 (2003) 1496-1506.
- [17] K. Svanberg, The method of moving asymptotes - a new method for structural optimization, *Int. J. Numer. Meth. Engng.*, 24 (1987) 359-373.